PHILOSOPHICAL TRANSACTIONS OF THE ROYAL SOCIETY A MATHEMATICAL, PHYSICAL & ENGINEERING SCIENCES

An adiabatic model for calculating overtone spectra of dimers such as $(H_2O)_2$

J. Tennyson, M. J. Barber and R. E. A. Kelly

Phil. Trans. R. Soc. A 2012 **370**, 2656-2674
doi: 10.1098/rsta.2011.0243

PHILOSOPHICAL TRANSACTIONS OF THE ROYAL SOCIETY A

Phil. Trans. R. Soc. A (2012) **370**, 2656–2674
doi:10.1098/rsta.2011.0243

An adiabatic model for calculating overtone spectra of dimers such as $(H_2O)_2$

By J. Tennyson*, M. J. Barber and R. E. A. Kelly

Department of Physics and Astronomy, University College London, London WC1E 6BT, UK

The near-infrared and visible wavelength spectrum of the water dimer is considered to be the major contributor to the so-called water continuum at these wavelengths. However, theoretical models of this spectrum require the simultaneous treatment of both monomer and dimer excitations. A model for treating this problem is proposed which is based upon a Franck–Condon-like separation between the monomer and dimer vibrational motions. In this model, one of the monomers is treated as the chromophore and its absorption is assumed to be given by its, possibly perturbed, vibrational band intensity. The main computational issue is the treatment of separate monomer and dimer motions. Various approaches for obtaining dimer vibration–rotation tunnelling spectra that allow for monomer motion are explored. These approaches include ways of treating the adiabatic separation of dimer vibrational modes from monomer vibrational modes. We classify the adiabatic separation methods under four main approaches: namely *fixed-geometry*, *free-monomer*, *perturbed-monomer* and *coupled-monomer* methods. The latter being the most computationally expensive as the monomer wave functions are dependent on the dimer coordinates. For each of these approaches, expectation values over the full potential are calculated for the given monomer vibrational wave functions. Various full (named VAP $2p$D in the text) and partial (VAP $(+p)$D) averaging techniques are outlined to calculate the vibrationally averaged, monomer state-dependent, dimer interaction potentials. The computational costs associated with application of these techniques to the water dimer are estimated and the prospects for full calculations based on this approach are assessed.

Keywords: water dimer; water continuum; Franck–Condon; potential energy surface; dipole moment surface

1. Introduction

The absorption of water dimers at near-infrared and visible wavelengths is extremely topical because of their importance for the atmospheric water continuum [1,2]. In this work, we propose a theoretical model for addressing this issue from first principles.

The absorption of light by dimers at microwave and far-infrared wavelengths has been well studied both experimentally and theoretically. From a theoretical point of view, spectroscopic studies in this region can generally be simplified

*Author for correspondence (j.tennyson@ucl.ac.uk).

One contribution of 17 to a Theo Murphy Meeting Issue ‘Water in the gas phase’.

by assuming that the modes being excited are purely dimer ones and therefore significant changes in the monomer configuration need not be considered. However, modelling the absorption properties of dimers at near-infrared and visible wavelengths is much less straightforward. The absorption of a high-frequency photon presents a much more demanding problem as the majority of the energy gained by the system will inevitably end up in one of the monomers. Indeed, it is likely that for such absorptions, the monomer will act as the main chromophore for the process with the dimer modes providing fine structure for any transition. Under these circumstances, any theoretical model has to consider both the motions of the monomer, and how these motions couple with the dimer motions.

For definiteness, we consider only dimers formed between similar species. Consider such a dimer formed by two nonlinear N-atomic molecules. The dimer will have $6N-6$ vibrational modes which can be partitioned as $3N-6$ ($=p$, later) vibrational modes associated with each monomer and six dimer modes. It would seem that to treat the situation where a monomer is vibrationally excited in a spectrum, it would be necessary to treat at least $3N$ and possibly all $6N-6$ modes simultaneously. However, this is undesirable, not only because of the huge computational cost of such an undertaking for all but a few simple systems, but also because the weak binding between most dimers means that a monomer vibrational excitation contains enough energy to dissociate the dimer. In other words, the monomer excitation lies in the continuum of the dimer states. The coupling between these modes is important for studies of pre-dissociation [3] but an additional complication one would want to avoid in calculating a simple absorption spectra.

A full-dimensional and computationally feasible solution to the dimer nuclear motion problem is provided by diffusion Monte Carlo methods [4–6]. However, these are only really useful for a few very low-lying states because of the inability of the method to correctly predict nodal structures in wave functions. On the other hand, adiabatic separation methods that have been applied for some smaller polyatomic clusters exist [7–10]. In particular, methods such as MULTIMODE by Bowman *et al.* [11–13] and the harmonically coupled anharmonic oscillator methods by Kjaergarrd *et al.* [8,14–18] have been used to describe vibration–rotation–tunnelling (VRT) states in small polyatomic clusters including the water dimer. These methods decouple the modes to make the calculations tractable. However, to improve on our current understanding of the water continuum, new spectroscopic methods and high-quality potential energy surfaces are necessary to probe the vibrational fine structure induced by the transitions between dimer states from excited monomers. For example, using the harmonically coupled anharmonic oscillator method to predict absorption for the water dimer [15] produces features which are not observed experimentally [19,20].

Some time ago, Brocks *et al.* [21] derived a general Hamiltonian for treating the nuclear motion problem given by molecule A forming a dimer with molecule B. This Hamiltonian assumes, for purposes of defining the kinetic energy operator, that molecules A and B keep their own identity in forming the cluster, but is otherwise perfectly general. This Hamiltonian has subsequently been widely used as the basis for treating dimer nuclear motion problems such as those implied by the atmospherically important water dimer [9,10,22–34] and other polyatomic dimers [35,36].

In this paper, we discuss strategies for treating the dimer overtone problem by partitioning the problem along lines similar to the work of Brocks *et al.* Key to this strategy is a Franck–Condon-like treatment of the overtone spectrum and a final nuclear motion problem that requires only the treating of the six dimer vibrational modes. The appropriate kinetic energy operators are thus provided by the Hamiltonian of Brocks *et al.* and the question comes down to the choice of (i) separation between monomer and dimer modes, (ii) characterization of the chromophore and its band intensity, and (iii) an appropriate potential energy function to be used for the dimer. Here, we make suggestions for each of these and, in particular, consider a number of possible ways of computing effective six-dimensional dimer potentials that allow for the monomer motions. This step tends to dominate the computation, so methods are assessed according to their computational cost and their efficacy for the water dimer problem.

2. A Franck–Condon-like model for the overtone spectrum

The line strength for a transition from dimer state m to dimer state n can be written

$$S(m-n) = |\langle m|\boldsymbol{\mu}|n\rangle|^2, \tag{2.1}$$

where the wave functions in the bra-ket are for all $6N-6$ dimer vibrational modes of the upper and lower state, respectively, plus the three modes associated with the rotation of the whole molecule and $\boldsymbol{\mu}$ is the appropriate dipole moment.

The p-dimensional monomer coordinates within the dimer can be labelled as $\mathbf{Q}_A$ and $\mathbf{Q}_B$, and the six dimer coordinates $\mathbf{R}$. In the Hamiltonian of Brocks *et al.* [21], these dimer modes correspond to three Euler angles for each monomer ($\{\alpha_1, \beta_1, \gamma_1\}$ and $\{\alpha_2, \beta_2, \gamma_2\}$) and a distance R between the centre-of-mass of each molecule. However, only five of the Euler angles are required to describe the orientation of one monomer with respect to the other.

Our model starts by making an adiabatic separation of dimer and monomer modes, and therefore, assuming that one can distinguish between the modes in each of the monomers, the six dimer internal vibrations and the overall rotations. In this case, expression (2.1) can be re-written

$$S(m-n) = H_{mn}|\langle i_m|\langle j_m|\langle d_m|\boldsymbol{\mu}|d_n\rangle|j_n\rangle|i_n\rangle|^2, \tag{2.2}$$

where $|i\rangle$ and $|j\rangle$ are the wave functions of monomers A and B, respectively, and $|d\rangle$ are the dimer internal coordinates. How these wave functions can be best determined is considered in the next section. H_{mn} is a factor representing the overall rotation. These factors are usually known as Hönl–London factors. In reality, the overtone spectra we wish to consider are not rotationally resolved at atmospheric temperatures and pressures. This term is therefore likely to be replaced by a rotational band parameter in practical calculations.

For high overtone spectra, it is likely that the transition intensity for photon absorption is dominated by the transition within a single monomer. This is particularly true of a molecule like the water dimer as water monomer has strong absorption features all the way through the infrared and well into the visible.

With this assumption, one can rewrite equation (2.2) as

$$\begin{aligned} S(m-n) &= H_{mn}|\langle i_m|\boldsymbol{\mu}|i_n\rangle\langle j_m|j_n\rangle\langle d_m|d_n\rangle|^2 \\ &= H_{mn}|\langle i_m|\boldsymbol{\mu}|i_n\rangle|^2|\langle j_m|j_n\rangle|^2|\langle d_m|d_n\rangle|^2, \end{aligned} \tag{2.3}$$

where it has been assumed that monomer A, represented by wave function $|i\rangle$, acts as the chromophore. If this is true, then monomer B is unchanged by the transition meaning $|j_m\rangle = |j_n\rangle$ and $|\langle j_m|j_n\rangle|^2 = 1$.

This yields our final expression for the transition intensity of an overtone band:

$$S(m-n) = |\langle i_m|\boldsymbol{\mu}|i_n\rangle|^2|\langle d_m|d_n\rangle|^2, \tag{2.4}$$

where $|\langle d_m|d_n\rangle|^2$ is the overlap of dimer modes between dimers whose monomers are in different vibrational states. This term is our equivalent of a Franck–Condon factor and accounts for the vibrational fine structure in a given overtone band. The expression (2.4) neglects the rotational fine structure. The underlying intensity of the transition is given by the monomer vibrational band intensity $|\langle i_m|\boldsymbol{\mu}|i_n\rangle|^2$. The following sections discuss possible ways of calculating these various terms.

Our Franck–Condon model neglects, or at least approximates, couplings between the different classes of modes within the dimer represented by $|d\rangle$, $|i_A\rangle$ and $|j_B\rangle$. One can expect this separation to become more reliable as the degree of excitation of the monomer increases. Thus, our model should be best at representing dimer absorption at near-infrared and visible wavelengths. However, the dipole moment changes significantly in the dimer environment and therefore $\boldsymbol{\mu}$ used to calculate the mononer vibrational band intensity cannot be simply that of the isolated monomer. This issue is explored below.

3. Effective potentials

(*a*) *Potential averaging*

In order to perform the adiabatic separation discussed above, one requires an effective, six-dimensional interaction potential, $V^{6D}_{\mathrm{eff},i_Aj_B}(\mathbf{R})$, which is calculated as the expectation value of the global, $(6N-6)$-dimensional potential, $V_{\mathrm{full}}(\mathbf{Q}_A, \mathbf{Q}_B; \mathbf{R})$, at each $\mathbf{R}$ grid point

$$V^{6D}_{\mathrm{eff},i_Aj_B}(\mathbf{R}) = \langle i_Aj_B|\, V_{\mathrm{full}}(\mathbf{Q}_A, \mathbf{Q}_B; \mathbf{R})|i_Aj_B\rangle \tag{3.1}$$

for monomer vibrational states $|i_A\rangle$ and $|j_B\rangle$. The monomer wave functions are solutions of the rotationless problem

$$\{\hat{T}_A + \mathbf{V}(\mathbf{Q}_A, \mathbf{Q}^0_B; \mathbf{R})\}\psi_A = E_A\psi_A \tag{3.2}$$

and

$$\{\hat{T}_B + \mathbf{V}(\mathbf{Q}^0_A, \mathbf{Q}_B; \mathbf{R})\}\psi_B = E_B\psi_B \tag{3.3}$$

with an appropriate choice of potential; $\mathbf{Q}^0_A$ and $\mathbf{Q}^0_B$ are appropriate reference geometries which will be discussed further below. This leads to a set of (i_Aj_B) monomer vibrational state-dependent effective potentials which are the input for six-dimensional dimer nuclear motion calculations.

The definition of $V^{6D}_{\mathrm{eff},i_Aj_B}(\mathbf{R})$ in equation (3.1) is far from unique as there are choices that have to be made about (i) the definition of the monomer vibrational wave functions and (ii) the actual averaging procedure. Possibilities for the definition of the vibrational wave functions include the following.

1. The *fixed-geometry* approach where one uses fixed monomer coordinates in the potential evaluation. Rather than averaging the potential, the potential is evaluated at vibrationally averaged geometries

$$V^{6D}_{\mathrm{eff},i_Aj_B}(\mathbf{R}) = V_{\mathrm{full}}(\langle i_A|\mathbf{Q}_A|i_A\rangle, \langle j_B|\mathbf{Q}_B|j_B\rangle; \mathbf{R}) \tag{3.4}$$

   instead. The approach has been widely recommended for studying the dimers formed by two monomers in their vibrational ground state ($\mathbf{Q}^0$). However, it is less obvious that this approach is appropriate for vibrationally excited monomers. We label this method fixed-geometry VGS (for vibrational ground state). One may also use the equilibrium geometry $\mathbf{Q}^{\mathrm{e}}$ for such studies. The use of the equilibrium geometry is, of course, only useful for systems where the monomers are not excited. We label this method fixed-geometry EQ (for equilibrium geometry).
2. The *free-monomer* approach uses the same unperturbed (free) monomer wave functions at every point. Full-averaging over monomer internal coordinates $\mathbf{Q}_A$ and $\mathbf{Q}_B$ means treating monomer states $|i_A\rangle$ and $|j_B\rangle$ simultaneously. These states are not $\mathbf{R}$-dependent: the free monomer wave functions are calculated for the potential with $R = \infty$, which may be say $100.0a_0$ for practical purposes.
3. The *perturbed-monomer* approach: as the monomer wave functions are influenced by the dimer environment, a simple improvement to the free-monomer approach is to use monomer wave functions computed as some fixed dimer geometry. Here, the monomer wave functions are calculated for the potential with $\mathbf{R} = \mathbf{R}^{\mathrm{min}}$, or one may consider some other cut through the full potential.
4. The *coupled-monomer* approach where the perturbed monomer wave functions are calculated at each $\mathbf{R}$ point.

Once the monomer wave functions have been calculated using one of the approaches 2, 3 or 4 above, the next consideration is how to perform the average over the calculated states. Two choices exist.

1. Creating a $(2p)$D vibrational averaged potential (VAP) which requires averaging over monomer internal coordinates $\mathbf{Q}_A$ and $\mathbf{Q}_B$ for monomer states $|i_A\rangle = \psi^i_A$ and $|i_B\rangle = \psi^j_B$ simultaneously:

$$\begin{aligned}&\langle i_Aj_B|\, V^{6D}_{\mathrm{full}}(\mathbf{Q}_A, \mathbf{Q}_B; \mathbf{R})\,|i_Aj_B\rangle \\ &\quad = \sum_{\mathbf{Q}_A,\mathbf{Q}_B} |\psi^i_A(\mathbf{Q}_A)|^2 |\psi^j_B(\mathbf{Q}_B)|^2\, V_{\mathrm{full}}(\mathbf{Q}_A, \mathbf{Q}_B; \mathbf{R}),\end{aligned} \tag{3.5}$$

   where the monomer wave functions are assumed to be normalized.

2. $(p+p)$D VAP where one expands the six-dimensional interaction potential at $\mathbf{R}$ to first order:

$$\langle i_A j_B|\, V^{6\mathrm{D}}_{\mathrm{full}}(\mathbf{Q}_A,\mathbf{Q}_B;\mathbf{R})|i_A j_B\rangle = \langle i_A|\, V_{\mathrm{full}}(\mathbf{Q}_A,\mathbf{Q}^0_B;\mathbf{R})|i_A\rangle + \langle j_B|\, V_{\mathrm{full}}(\mathbf{Q}^0_A,\mathbf{Q}_B;\mathbf{R})|j_B\rangle - V_{\mathrm{full}}(\mathbf{Q}^0_A,\mathbf{Q}^0_B;\mathbf{R}), \tag{3.6}$$

which involves averaging over monomer internal coordinates $\mathbf{Q}_A$ and $\mathbf{Q}_B$ for monomer states ψ^i_A and ψ^j_B separately. This is only a partial averaging scheme as the averaging is performed over each molecule separately and so it is only an approximation to the full adiabatic separation method. The expansion point for each monomer may be chosen as $\mathbf{Q}_X = \mathbf{Q}^0$, $\mathbf{Q}^{\mathrm{e}}$ or $\mathbf{Q}^{\mathrm{min}}$. The first approach is probably the most physically accurate. The first two choices require less computation as they are not $\mathbf{R}$-dependent, although one may consider computing the vibrationally averaged ground state geometry to be computed at each $\mathbf{R}$-point. Leforestier [10], for example, expanded around $\mathbf{Q}^{\mathrm{min}}$, which is chosen as the minimum, i.e. similar to using $\mathbf{Q}^{\mathrm{e}}$, but for the dimer configuration under consideration.

What is generally required for dimer VRT level calculations is the interaction potential defined as the energy of the system minus the energy of the parts in the same state. The expression for the actual effective potential, as given by equation (3.1), must therefore be adjusted to give the effective interaction potential:

$$V^{6\mathrm{D}}_{\mathrm{int},i_A j_B}(\mathbf{R}) = \langle i_A j_B|\, V_{\mathrm{full}}(\mathbf{Q}_A,\mathbf{Q}_B;\mathbf{R})|i_A j_B\rangle - \langle i'_A j'_B|\, V_{\mathrm{full}}(\mathbf{Q}_A,\mathbf{Q}_B;\infty)|i'_A j'_B\rangle, \tag{3.7}$$

where $V_{\mathrm{full}}(\mathbf{Q}_A,\mathbf{Q}_B;\infty)$ is the energy of the dissociated dimer. The total energy requires the monomer excited states $|i'_A\rangle$ and $|j'_B\rangle$ to be calculated for monomers A and B, respectively. Since, generally, the monomers relax in the dimer environment, the monomer states $|i_A\rangle$ and $|j_B\rangle$ are usually not equal to $|i'_A\rangle$ and $|i'_B\rangle$, respectively. The exception is when the free monomer wave functions are used to average the potential on the dimer grid in the free-monomer approach. This approach has been used by us previously for the water dimer [37]. In practice, we found that actual water dimer potentials were less numerically stable for excitation of both monomers at large distance. Therefore, it was necessary to expand the reference energy to obtain

$$\langle i'_A j'_B|\, V^{6\mathrm{D}}_{\mathrm{full}}(\mathbf{Q}_A,\mathbf{Q}_B;\infty)|i'_A j'_B\rangle = \langle i'_A|\, V_{\mathrm{full}}(\mathbf{Q}_A,\mathbf{Q}^0_B;\infty)|i'_A\rangle + \langle j'_B|\, V_{\mathrm{full}}(\mathbf{Q}^0_A,\mathbf{Q}_B;\infty)|j'_B\rangle - V_{\mathrm{full}}(\mathbf{Q}^0_A,\mathbf{Q}^0_B;\infty), \tag{3.8}$$

which gave a more numerically stable expression for the interaction energy.

(*b*) *Corrections to the potential*

As implied above, the potential energy surface (PES) for a dimer can be considered to comprise three terms: potentials owing to the isolated monomers, an interaction potential between the two frozen dimers and the remaining cross

terms. It is usually possible to obtain much more accurate PESs for the monomer and dimer interaction terms. These can be incorporated into a full PES as corrections. In particular, creating overtone spectra for dimers requires a potential which accurately describes the monomer motion. To correct any dimer potential, one may add corrections [37,38] for each monomer $\delta V^{\mathrm{M}}(\mathbf{Q}_A)$ and $\delta V^{\mathrm{M}}(\mathbf{Q}_B)$ as well as a possible correction for the six-dimensional dimer PES, $\delta V^{\mathrm{6D}}(\mathbf{R})$. These are included as

$$V_{\mathrm{full}}(\mathbf{Q}_A,\mathbf{Q}_B,\mathbf{R}) = V_{\mathrm{approx}}(\mathbf{Q}_A,\mathbf{Q}_B,\mathbf{R}) + \delta V^{\mathrm{M}}(\mathbf{Q}_A) + \delta V^{\mathrm{M}}(\mathbf{Q}_B) + \delta V^{\mathrm{6D}}(\mathbf{R}), \tag{3.9}$$

where

$$\delta V^{\mathrm{M}}(\mathbf{Q}_A) = V(\mathbf{Q}_A) - V(\mathbf{Q}^{\mathrm{e}}) - [V_{\mathrm{approx}}(\mathbf{Q}_A,\mathbf{Q}_B^{\mathrm{e}},\infty) - V_{\mathrm{approx}}(\mathbf{Q}_A^{\mathrm{e}},\mathbf{Q}_B^{\mathrm{e}},\infty)] \tag{3.10}$$

and

$$\delta V^{\mathrm{M}}(\mathbf{Q}_B) = V(\mathbf{Q}_B) - V(\mathbf{Q}^{\mathrm{e}}) - [V_{\mathrm{approx}}(\mathbf{Q}_A^{\mathrm{e}},\mathbf{Q}_B,\infty) - V_{\mathrm{approx}}(\mathbf{Q}_A^{\mathrm{e}},\mathbf{Q}_B^{\mathrm{e}},\infty)]. \tag{3.11}$$

The monomer corrections predict much better band origins when compared with experiment, as well as providing a more accurate barrier to linearity [37,38]. Note that the $\mathbf{Q}^{\mathrm{e}}$ geometry corresponds to the minimum on the monomer surface, which is not the same as the monomer minimum on the full dimer surface. The monomer minimum must be used in the corrections for them to be consistent.

In the free-monomer and perturbed-monomer methods, the monomer states are not **R**-dependent, so that $\langle i_A|\delta V^{\mathrm{3D}}(\mathbf{Q}_A)|i_A\rangle$ and $\langle j_B|\delta V^{\mathrm{3D}}(\mathbf{Q}_B)|j_B\rangle$ can be calculated once and added *a posteriori* to the interaction potential. In the free-monomer approach, the monomer corrections in the interaction energy expression simply cancel so that one only needs to average the original, uncorrected PES [37].

In contrast, in the coupled-monomer method, the monomer corrections must be calculated at each dimer grid point as the states themselves are **R**-dependent.

A dimer correction may also be desirable since a better six-dimensional dimer potential may exist, which is able to describe more accurately the stationary points as well as the dimer vibration–rotation states [32]. The dimer correction takes the form

$$\delta V^{\mathrm{6D}}(\mathbf{R}) = V^{\mathrm{6D}}(\mathbf{R}) - V^{\mathrm{12D}}(\mathbf{Q}_1^0,\mathbf{Q}_2^0,\mathbf{R}). \tag{3.12}$$

This correction is independent of the monomer wave functions ψ_A^i and ψ_B^j and so can be added after the averaging has been performed.

(*c*) *Computational considerations*

For simplicity, we assume that the monomer wave functions can be generated reasonably quickly on a grid, such as one given by a discrete variable representation (DVR) procedure. Below, we assume that m grid points are required to specify each monomer wave function and a grid of M points are needed to specify the effective six-dimensional potential for dimer nuclear motion calculations. Table 1 gives illustrative numbers for the case of the water dimer,

where a dimer grid of $M = 2\,893\,401$ has been found to be adequate in previous studies [34] and monomer grids based on the number of radial grid points (n_r) and number of angular points (n_θ), which are needed depending on the range of excited states to be considered. For water $m = n_\theta n_r^2$ or $n_\theta(n_r/2)(n_r + 1)$ if symmetry is used.

(i) *The geometrically averaged approach*

The coordinate averaging required by this approach is straightforward and takes much less computer time than the potential averaging methods discussed below.

(ii) *The free-monomer approach*

In the free-monomer approach, the monomer eigenproblem is solved once. The potential is averaged over the unperturbed monomer wave functions of the monomers at each dimer grid point, so that we have m^2 potential evaluations for each of the M dimer points for the full averaging; and $2m$ potential evaluations for each dimer point in the partial-averaging scheme. It should be noted that the averaging calculations at each dimer grid point are completely independent from one another, which is an ideal case for grid computing.

From the above analysis, it is clear the partial-average method is significantly cheaper, both in time and memory requirements. As can be seen from table 1, any attempt to store all of the potential points with the full approach would be unfeasible. To avoid storing these, the *full* six-dimensional averaging can be performed *on-the-fly* at each dimer point, $\mathbf{R}_i$. All the potential evaluations $V_{\text{full}}(\mathbf{Q}_A, \mathbf{Q}_B, \mathbf{R}_i)$ are then discarded and only the averaged points, $V^{6D}_{\text{eff},i_A j_B}(\mathbf{R}_i)$, stored. This method has the disadvantage that it only allows limited *a posteriori* adjustments to the potential. However, in this scheme, the memory required for each average becomes quite small, shown by the space required per point in table 1. We have implemented a procedure for performing these calculations using the CONDOR [39,40] protocol which allows the effective interaction potential calculations at each dimer grid point to be evaluated in a completely delocalized fashion across a large number of essentially uncoupled personal computers.

(iii) *The perturbed-monomer approach*

From a computational perspective, perturbed-monomer calculations are a straightforward generalization of the free-monomer approach above with the possible exception of symmetry considerations. If the monomers are in the same vibrational state, say the vibrational ground state ($|00\rangle$), then there is a clear interchange symmetry between the two monomers. However, if one monomer is excited, then whether there is symmetry between $|i0\rangle$ and $|0i\rangle$ depends on the time scale for interchange between the two dimers. Experience with the water dimer, where the two monomers exist in different environments, suggests this interchange between the two to be much less significant [41], so that we do not consider it here. This leads to a significant reduction in symmetry with consequent increase in computer resources. In the case of the water dimer, the symmetry drops from G_{16} to G_4. The extra couplings implied by this reduction in symmetry have not

Table 1. Computational costs of six-dimensional and (3 + 3)-dimensional averaging in the *free-monomer* approach. Various monomer grids are shown based on the example of the water dimer.

			six-dimensional approach					(3 + 3)-dimensional approach				
reliability energy	monomer basis		potential calls		space		time	potential calls		space		time
(cm^{-1})	n_r	θ	per point	total	point (MB)	total (TB)	(days)	per point	total	point (KB)	total (GB)	(days)
3755.6	6	18	142 884	4.134×10^{11}	1.1	3.3	829	378	2.187×10^{9}	3.0	8.7	4.4
5331.2	6	19	159 201	4.606×10^{11}	1.2	3.7	924	399	2.309×10^{9}	3.2	9.2	4.6
6871.5	6	20	176 400	5.104×10^{11}	1.4	4.1	1024	420	$\times 10^{9}$	3.4	9.7	4.9
11 242.7	7	24	451 584	1.307×10^{12}	3.6	10.5	2622	672	$\times 10^{9}$	5.4	15.5	7.8
13 453.5	7	26	529 984	1.533×10^{12}	4.2	12.3	3077	728	$\times 10^{9}$	5.8	16.8	8.5
13 660.3	8	26	876 096	2.534×10^{12}	7.0	20.3	5086	936	$\times 10^{9}$	7.5	21.7	10.9
16 546.3	9	32	2 073 600	6.000×10^{12}	16.6	48.0	12 038	1440	$\times 10^{9}$	11.5	33.3	16.7
18 332.1	12	29	5 116 644	1.480×10^{13}	40.9	118.4	29 703	2262	$\times 10^{9}$	18.1	52.6	26.6
19 781.2	15	29	12 110 400	3.504×10^{13}	96.9	280.3	70 304	3480	$\times 10^{9}$	27.8	80.6	40.4
26 000	29	40	302 760 000	8.760×10^{14}	2422.1	7008.0	1 757 598	17 400	$\times 10^{9}$	139.2	402.8	202.0

always been included in practical calculations [10]. In this reference, the donor–acceptor interchange was not permitted but (at variance with our method) the donor hydrogen interchange was, resulting in G_8 symmetry.

(iv) *The coupled-monomer approach*

This approach uses the solution of the monomer eigenproblems at each dimer grid point, $\mathbf{R}_i$. The procedure requires:

— fixing the geometry of monomer A at some reference geometry Q_A^0, such as the vibrational ground state geometry, $\langle 0|\, Q_A|0\rangle$. This avoids the additional expense of performing the minimization calculations at each dimer grid point [10]. One can then solve the eigenproblem for monomer B;
— calculate the expectation value of the potential for all states $|0_A j_B\rangle$; and
— repeat for monomer A with B frozen.

Solving the monomer eigenproblems at infinity and calculating the averaged potential at infinity for all states $|i_A 0_B\rangle$ and $|0_A j_B\rangle$ need only be performed once.

The calculation of the wave functions at each point comes at a significant additional cost: for the water acceptor calculations, $2\,893\,401 \times \sim 1\,\mathrm{s} = 33$ CPU days are required; and the donor calculations require much longer at around $2\,893\,401 \times 14\,\mathrm{s} = 469$ CPU days. We implemented an algorithm which performs each of the required steps distributed across University College London's Legion high-performance computing service. Again, we performed the averaging *on-the-fly* and the calculations took around three weeks on approximately 600 CPUs. The additional cost of full six-dimensional averaging approximately doubles the computational requirements. Therefore, the $(3+3)$-dimensional-averaging method has a significant computational advantage.

4. Methodology

(*a*) *Water dimer nuclear motion*

For actual calculations on the water dimer, we use the full-dimensional HBB2 potential [42] with a monomer correction given by the Shirin *et al.* [43] water potential (SHI08). The $\mathbf{Q}^{\mathrm{e}}$ geometry corresponds to the minimum on the SHI08 surface, which is not the same as the monomer minimum on the HBB surface. The SHI08 minimum must be used in the corrections for them to be consistent.

A dimer correction was not included as calculations involving corrections to the HBB2 surface with the highly accurate six-dimensional CCpol8s dimer PES owing to Cencek *et al.* [32] were problematic because of the calculations being performed with the monomers in the vibrational ground state geometry: this introduced a double-counting correction error, when combined with the monomer correction, for the monomer motion.

For all methods, the effective potentials come from vibrationally averaging over DVR3D [44] wave functions for the water monomers. The software uses a DVR grid based on a number of radial points, n_{r}, and angular points, n_θ. For energy levels up to $20\,000\,\mathrm{cm}^{-1}$, values of $n_{\mathrm{r}} = 29$ and $n_\theta = 40$ have been shown to give highly accurate results [43,45,46]. However, to reduce the cost of computation of

the expectation values, we have shown that changing the Morse parameters and reducing the basis can give good results up to 12 000 cm^{-1} for values of $n_r = 7$ and $n_\theta = 24$ [37].

The calculation of the dimer VRT levels is performed using the Hamiltonian of Brocks *et al.* [21]. The methodology is explained in some detail by Groenenboom *et al.* [23], and so only briefly covered here. An angular basis constructed as a direct product of rotor functions is employed for both the monomer rotations, $D^{(j_A)*}_{m_A k_A}$ and $D^{(j_B)*}_{m_B k_B}$, where j_X corresponds to the angular momenta of monomer X, and $D^{(J)*}_{MK}$ to the overall dimer rotation. For H_2O, energy convergence of the dimer levels was found for a j_X^{max} value of 11 [23]. However, for the excited state calculations, the j_X^{max} value had to be reduced to 8 to make the calculations possible.

The effective potential is given as an expansion over rotor functions in the angular coordinates [23] up to some maximum values of L_X. These are truncated to $L_X^{max} = 8$, which has been shown to give good convergence to the full problem [23]. The angular integrals required to compute the R-dependent coefficients in the expansion of the potential are performed using $L_A^{max} + 1$ quadrature points in each coordinate: $L_A^{max} + 1$ point Gauss–Legendre quadrature is used for β_1 and β_2, while $2L_A^{max} + 1$ point Gauss–Chebychev quadrature is used for $\alpha_1 - \alpha_2$, γ_1 and γ_2. For the Gauss–Chebychev grid, symmetry implies that only $L_A^{max} + 1$ potential calls are actually needed.

Three contracted DVR functions are necessary for the radial basis to get well-converged energies [23]. The DVR grid contains $n_R = 49$ points between 4 and $9a_0$. A single, well-converged six-dimensional dimer calculation requires the evaluation of a total of $n_R(L_A^{max} + 1)^5 = 2\,893\,401$ potential points.

When the monomers are in their vibrational ground states, tunnelling of the atoms in the water dimer takes the form: (a) acceptor tunnelling, (b) donor–acceptor interchange, and (c) donor bifurcation tunnelling, leading to splittings in the observed spectra of the water dimer. The permutation-inversion group G_{16} may be used here with irreducible elements $A_1^\pm$, $A_2^\pm$, $B_1^\pm$, $B_2^\pm$ and $E^\pm$, which are used to label the water dimer VRT energy levels with non-excited monomers.

For the excited state calculations, we use G_4 symmetry which only regards the hydrogen interchange on the acceptor unit as a feasible tunnelling mechanism.

(*b*) *Vibrational band intensities*

The monomer vibrational band intensity, $\langle i_m|\mu|i_n\rangle$, required by equation (2.4) can be evaluated using fairly standard theory. Following Le Sueur *et al.* [47], the dipole moments are rotated into Eckart coordinates and evaluated using the program DIPJ0 [48], which calculates vibrational band intensities within the framework of DVR3D. However, the real issues are (i) what are the appropriate monomer wave functions to use and (ii) what dipole surface should one use?

The obvious choice in monomer wave functions is between free-monomer wave functions and ones perturbed by the dimer environment. Given that the dimer environment provides a contribution to overall dipole moment and that the two water monomers experience rather different perturbations owing to the dimer, unperturbed wave functions are unlikely to yield good results.

By the same logic, although there are very good dipole surfaces available for the water monomer [49,50], these cannot be used unaltered for dimer calculations. In this work, we use the full-dimensional, *ab initio* dipole moment surface of Wang *et al.* [42] corrected using the high-accuracy, *ab initio* monomer CVR dipole surface of Lodi *et al.* [49] in a manner analogous to the potential corrections discussed above.

5. Results

Seven sets of results are given for the techniques outlined below.

1. *Fixed-monomer* EQ method where the monomer units are fixed in the equilibrium geometry, $\mathbf{Q}^{e}$.
2. *Fixed-monomer* VGS where the water units are fixed at $\mathbf{Q}^{0}$. This is the normal approach to solve the dimer problem when both monomers are in their ground state.
3. *Free-monomer* VAP six-dimensional approach uses unperturbed monomer wave functions with full six-dimensional averaging.
4. *Free-monomer* VAP $(3+3)$-dimensional/EQ approach uses partial averaging with an expansion point for the perturbation from the other monomer (when averaged) fixed at the EQ geometry.
5. *Free-monomer* VAP $(3+3)$-dimensional again uses partial averaging but with the expansion point being the VGS geometry. The VGS notation is dropped as this is the standard $(3+3)$-dimensional technique that we use in the following two methods.
6. *Perturbed-monomer* VAP $(3+3)$-dimensional approach which uses perturbed monomer wave functions with partial $(3+3)$-dimensional averaging.
7. *Coupled-monomer* VAP $(3+3)$-dimensional approach where we calculate the wave functions at each dimer grid point and again use only partial averaging to keep the calculations tractable.

The results of using these models on the accuracy of reproducing the observed parameters of the water dimer with the monomers in the ground state are summarized in table 2; results of the individual calculations are extensive and are available from the first author on request. It is clear that the *free-monomer* six-dimensional VAP method and the free-monomer VAP $(3+3)$-dimensional/GS approach are the worst in reproducing the band origins. However, all methods give a similar level of accuracy. This is true for the band origins, interchange splittings and rotational constants.

When compared with the results using the HBB+SHI08 [37], there is a marked improvement in the reproduction of the dimer vibrational band origins for the HBB2+SHI08 potential, seemingly at the expense of the rotational constants. The level of improvement to the band origins more than justifies the use of the newer potential. We note that the interchange splittings remain relatively unchanged.

The most accurate results are reported for the free-monomer VAP $(3+3)$-dimensional approach and the coupled-monomer method. This is to be expected as the free-monomer averaging approaches involve unperturbed wave functions.

Table 2. Standard errors (cm^{-1}) for the dimer vibrational band origins ($\sigma_{origins}$), interchange ($\sigma_{interchange}$) and rotational constants (σ_{rot}) for the various methods reported here applied to the water dimer with both monomers in their vibrational ground state. Results of Kelly *et al.* [37] for the HBB potential are also shown; this work details actual parameters calculated and their experimental values.

potential	method		$\sigma_{origins}$	$\sigma_{interchange}$	σ_{rot}
HBB + SHI08	fixed-geometry	EQ	10.25	1.49	0.01
		VGS	8.06	1.05	0.08
	free-monomer	VAP six-dimensional	8.27	0.89	0.19
HBB2 + SHI08	fixed-geometry	EQ	4.79	1.26	0.16
		VGS	2.89	1.15	1.19
	free-monomer	VAP six-dimensional	5.39	1.12	1.39
		VAP (3 + 3)-dimensional/EQ	4.56	1.19	1.07
		VAP (3 + 3)-dimensional	4.64	1.10	1.05
	perturbed-monomer	VAP (3 + 3)-dimensional	4.89	0.82	1.48
	coupled-monomer	VAP (3 + 3)-dimensional	3.89	1.19	0.79

The perturbed-monomer approach again will overestimate the dimer interaction as the same (highly) perturbed donor and acceptor wave functions are averaged across the dimer grid. The averaged geometry calculations may work better because rather than averaging over the potential itself (which will introduce small errors in the two examples above), we use an average value for the geometry where $\mathbf{Q}_A = \mathbf{Q}_B = \mathbf{Q}^0$. The averaged geometry calculations actually perform slightly better than the coupled-monomer method but only slightly. However, the latter method allows us to probe dimer spectra, where the monomers are excited, which is the aim of this work. Note that the free-monomer VAP (3 + 3)-dimensional/EQ and VAP (3 + 3)-dimensional results give very similar results here, in comparison with the fixed-geometry EQ and VGS results. However, this is to be expected as the averaging is performed on the vibrational ground state for each respective molecule.

In table 3, we give the fundamental stretching and bending transitions for all six water monomer vibrational states in the dimer. For comparison, we included the frequencies of these six modes calculated using HCAO and VPT2 methods from Kjaergaard *et al.* [18], as well as experimental values from matrix isolation and jet-cooled studies [41,51,52]. The *coupled-monomer* method seems to give reasonable results for the acceptor and donor bending modes, as well as the symmetric and asymmetric stretching modes on the acceptor and the free OH stretch on the donor. However, the results for the donor-bound OH stretching mode do not compare as well with the experiment as those given by the VPT2 study: the shift induced by the hydrogen bonding interaction is underestimated by around 43 cm^{-1} (on average). We suspect that this is because of the potential itself, as the monomer-corrected potential may affect the couplings between the monomer and dimer potentials, which will be particularly important for the bound OH stretch. It is worth noting that there is an improvement seen when compared with the HCAO study as the HOH-bending modes are reproduced to a much better accuracy here.

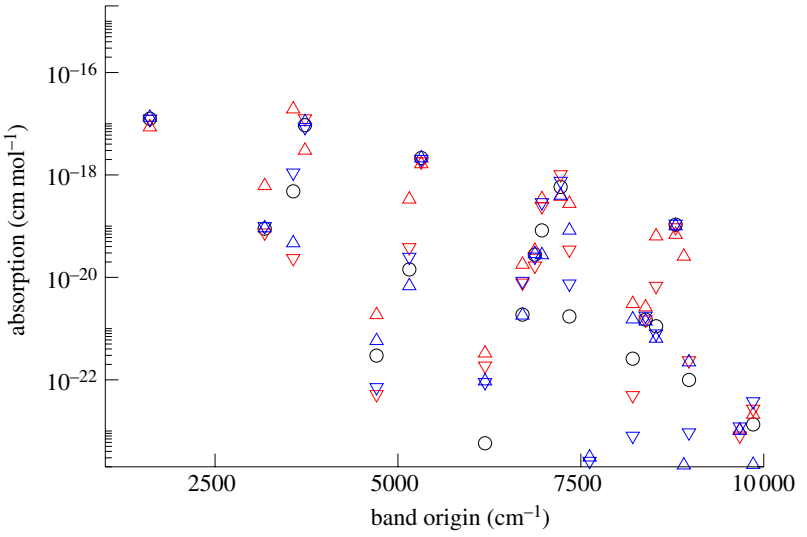

Figure 1. Calculated water monomer vibrational band intensities (see text for discussion of the models used). Circle, monomer; red upright triangle, donor (perturbed); red inverted triangle, acceptor (perturbed); blue upright triangle, donor (equilibrium); blue inverted triangle, acceptor (equilibrium). (Online version in colour.)

Table 3. Calculated frequencies of fundamental transitions in the water dimer: this work is based on the coupled-monomer method. Vibrational designations are as given by Kjaergaard *et al.* [18].

local mode	normal mode	this work	VPT2[a]	HCAO[a]	experiment
$\|0\rangle_f\|1\rangle_b\|0\rangle$	ν_3/ν_1 (d)	3640.8	3591	3565	3601[b]
$\|1\rangle_f\|0\rangle_b\|0\rangle$	ν_1/ν_3 (d)	3745.3	3711	3729	3735[b]
$\|10\rangle^+\|0\rangle$	ν_2/ν_1 (a)	3646.6	3634	3655	3660[b]
$\|10\rangle^-\|0\rangle$	ν_9/ν_3 (a)	3739.9	3725	3752	3745[c]
$\|0\rangle_f\|0\rangle_b\|1\rangle$	ν_4/ν_2 (d)	1599.6	1614	1662	1616[d]
$\|00\rangle\|1\rangle$	ν_5/ν_2 (a)	1597.2	1603	1642	1599[d]

[a]Adapted from Kjaergaard *et al.* [18].
[b]Adapted from Buck & Huisken [51].
[c]Adapted from Huang & Miller [41].
[d]Adapted from Bouteiller & Perchard [52]; similar results were obtained by Paul *et al.* [53].

Figure 1 compares vibrational band intensities calculated using various approximations for the dipole surface. As a benchmark, band intensities for the unperturbed monomer are given. These were calculated with the CVR dipole moment surface of Lodi *et al.* [49] and unperturbed monomer wave functions computed using the SHI08 potential energy surface. This calculation, as it makes no allowance for the dimer environment, gives identical intensities for absorption by the donor and acceptor water molecule.

The other models used a cut through the full dipole moment surface of the dimer. In the first case, this cut was taken for each (donor or acceptor) monomer with all other coordinates frozen at their equilibrium values. These results probably underestimate the effect of the dimer environment since this is not symmetric as the molecule vibrates about its equilibrium geometry. Some allowance is made for this in the perturbed model where cuts are taken through the dimer dipole moment surface with other geometric parameters frozen at their equilibrium values except for distance between the water monomer centre-of-masses, R, which was reduced by about 10 per cent to $5.3a_0$.

There remains very limited experimental data to be compared with our calculated band intensities. However, band water dimer cross sections have been measured by Paynter *et al.* [54] for the 1200–8000 cm^{-1} region. A comparison with this work suggests that around 1500 and 5400 cm^{-1} our band intensities are a little too weak. The band at around 3700 cm^{-1}, where the first stretches are significantly too weak, has also been studied in helium droplets [55]. However, the band at around 7200 cm^{-1} is in excellent agreement. This is consistent with the approximations in our basic Franck–Condon model which are likely to become more reliable as the level of excitation increases. We note that very recently work has been reported on absorption by the water dimer in a neon matrix that spans frequencies throughout the infrared [56]. This work will be used as the basis for future comparisons.

6. Conclusions

We propose a model for the calculation of dimer overtone spectra based on approaches for separating dimer from monomer motions within a binary complex. We analyse a number of methods of using this separation for calculating the rotation–vibration states of the water dimer as well as the intensity of the overtone transitions.

For the averaging approaches, we show that partial, or $(p + p)$D, approaches where the monomer vibrations are frozen in either the equilibrium or vibrational ground state geometry while averaging is performed on the other monomer's modes perform equally well as, if not better than, the full $2p$D averaging approach. Computationally, this is extremely important as this reduces a p^2 problem to a $2p$ one, which makes the donor and acceptor nuclear motion calculations at each dimer grid point tractable.

In addition, it can be seen that these *coupled-monomer* approaches reproduce the low-lying VRT levels to the best accuracy when compared with all the averaging approaches considered here. However, the VGS method, commonly used for dimer calculations when both monomers are in their vibrational ground state, performs slightly better in comparison. For excited monomer problems, for which the VGS method is not easily applicable, the *coupled-monomer* methodology should be even more important. However, the *perturbed-monomer* approach may provide a very good approximation to the coupled-monomer approach.

The fundamental bending and stretching transitions for the monomers in the dimer are well represented with the coupled-monomer method: the frequency shifts compare well with previous theoretical values and experiment. The exception being the bound OH mode which does not compare that well with

experiment and previous VPT2 calculations. We suspect this may be owing to the potential itself, since to obtain accurate shifts requires the dimer potential surface to be corrected for the monomer motion. This may adversely affect the couplings between the two potentials, particularly in the bound OH stretch mode.

Our objective is to augment the calculations presented here with solutions of the dimer problems involving excitation of one of the monomers. This is of particular importance for modelling the quasi-continuum atmospheric absorption owing to the water dimer at near-infrared and visible wavelengths. However, at atmospheric temperatures, it is necessary to consider every vibrational state of the dimer. This is a computationally challenging problem which is made more difficult by the loss of symmetry caused by the excitation of one of the dimers. Work is progressing in this direction.

We thank Gerrit J. Groenenboom and Ad van der Avoird for providing their dimer program, which we adapted for the calculations presented in this work, and for helpful discussions. We thank Xinchuan Huang, Yimin -M. Wang, Bastian J. Braams and Joel M. Bowman for providing us with the HBB potentials. We also acknowledge useful discussion with Henrik Kjaergaard, Andrei Vigasin and Lorenzo Lodi. The authors would also like to thank the NERC and EPSRC through the CAVIAR consortium for funding and also acknowledge the use of the UCL Research Computing Condor Pool, Legion and associated services in performing this work.

References

1 Gardiner, T. D., Coleman, M., Browning, H., Tallis, L., Ptashnik, I. V. & Shine, K. P. 2012 Absolute high spectral resolution measurements of surface solar radiation for detection of water vapour continuum absorption. *Phil. Trans. R. Soc. A* **370**, 2590–2610. (doi:10.1098/rsta.2011.0221)

2 Newman, S. M., Green, P. D., Ptashnik, I. V., Gardiner, T. D., Coleman, M. D., McPheat, R. A. & Smith, K. M. 2012 Airborne and satellite remote sensing of the mid-infrared water vapour continuum. *Phil. Trans. R. Soc. A* **370**, 2611–2636. (doi:10.1098/rsta.2011.0223)

3 Peet, A., Clary, D. C. & Hutson, J. M. 1986 Coupled channel calculations on the vibrational predissociation of the ethylene dimer. *Chem. Phys. Lett.* **125**, 477–480. (doi:10.1016/0009-2614(86)87083-X)

4 Anderson, J. A. 1975 A random-walk simulation of the Schrödinger equation. *J. Chem. Phys.* **63**, 1499–1503. (doi:10.1063/1.431514)

5 Anderson, J. A. 1976 Quantum chemistry by random walk. *J. Chem. Phys.* **65**, 4121–4127. (doi:10.1063/1.432868)

6 McCoy, A. B., Braams, B. J., Brown, A., Huang, X., Jin, Z. & Bowman, J. M. 2004 *Ab initio* diffusion Monte Carlo calculations of the quantum behaviour of CH_5^+ in full dimensionality. *J. Phys. Chem. A* **108**, 4991–4994. (doi:10.1021/jp0487096)

7 Cavagnat, D., Lespade, L. & Lapouge, C. 1995 Internal dynamics contributions to the CH stretching overtone spectra of gaseous monohydrogenated nitromethane NO_2CHD_2. *J. Chem. Phys.* **103**, 10 502–10 512. (doi:10.1063/1.469900)

8 Kjaergaard, H. G., Rong, Z. M., McAlees, A. J., Howard, D. L. & Henry, B. R. 2000 Internal methyl rotation in the CH stretching overtone spectra of toluene-α-d_2, -α-d_1, and -d_0. *J. Phys. Chem. A* **104**, 6398–6405. (doi:10.1021/jp000571d)

9 Leforestier, C., Gatti, F., Fellers, R. S. & Saykally, R. J. 2002 Determination of a flexible (12D) water dimer potential via direct inversion of spectroscopic data. *J. Chem. Phys.* **117**, 8710–8722. (doi:10.1063/1.1514977)

10 Leforestier, C., van Harrevelt, R. & van der Avoird, A. 2009 Vibration-rotation-tunneling levels of the water dimer from an *ab initio* potential energy surface with flexible monomers. *J. Phys. Chem. A* **113**, 12 285–12 294. (doi:10.1021/jp9020257)

11 Wang, Y., Carter, S., Braams, B. J. & Bowman, J. M. 2008 Multimode quantum calculations of intramolecular vibrational energies of the water dimer and trimer using *ab initio*-based potential energy surfaces. *J. Chem. Phys.* **128**, 071101. (doi:10.1063/1.2839303)

12 Wang, Y. & Bowman, J. M. 2010 Towards an *ab initio* flexible potential for water, and post-harmonic quantum vibrational analysis of water clusters. *Chem. Phys. Lett.* **491**, 1–10. (doi:10.1016/j.cplett.2010.03.025)

13 Carter, S., Sharma, A. R., Bowman, J. M., Rosmus, P. & Tarron, R. 2009 Calculations of rovibrational energies and dipole transition intensities for polyatomic molecules using MULTIMODE. *J. Chem. Phys.* **131**, 224106. (doi:10.1063/1.3266577)

14 Kjaergaard, H. G., Henry, B. R., Wei, H., Lefebvre, S. & Carrington, T. 1994 Calculation of vibrational fundamental and overtone band intensities of H_2O. *J. Chem. Phys.* **100**, 6228–6239. (doi:10.1063/1.467086)

15 Low, G. R. & Kjaergaard, H. G. 1999 Calculation of OH-stretching band intensities of the water dimer and trimer. *J. Chem. Phys.* **110**, 9104–9115. (doi:10.1063/1.478832)

16 Salmi, T., Hanninen, V., Garden, A. L., Kjaergaard, H. G., Tennyson, J. & Halonen, L. 2008 A calculation of the OH stretching vibrational overtone spectrum of the water dimer. *J. Phys. Chem. A* **112**, 6305–6312. (doi:10.1021/jp800754y)

17 Garden, A. L., Halonen, L. & Kjaergaard, H. G. 2008 Calculated band profiles of the OH-stretching transitions in water dimer. *J. Phys. Chem. A* **112**, 7439–7447. (doi:10.1021/jp802001g)

18 Kjaergaard, H. G., Garden, A. L., Chaban, G. M., Gerber, R. B., Matthews, D. A. & Stanton, J. F. 2008 Calculation of vibrational transition frequencies and intensities in water dimer: comparison of different vibrational approaches. *J. Phys. Chem. A* **112**, 4324–4335. (doi:10.1021/jp710066f)

19 Kassi, S., Macko, P., Naumenko, O. & Campargue, A. 2005 The absorption spectrum of water near 750 nm by CW-CRDS: contribution to the search of water dimer absorption. *Phys. Chem. Chem. Phys.* **7**, 2460–2467. (doi:10.1039/b502172c)

20 Shillings, A. J. L., Ball, S. M., Barber, M. J., Tennyson, J. & Jones, R. L. 2011 An upper limit for water dimer absorption in the 750 nm spectral region and a revised water line list. *Atmos. Chem. Phys.* **11**, 4273–4287. (doi:10.5194/acp-11-4273-2011)

21 Brocks, G., van der Avoird, A., Sutcliffe, B. T. & Tennyson, J. 1983 Quantum dynamics of non-rigid systems comprising two polyatomic molecules. *Mol. Phys.* **50**, 1025–1043. (doi:10.1080/00268978300102831)

22 Mas, E. M., Szalewicz, K., Bukowski, R. & van der Avoird, A. 1997 Pair potential for water from symmetry-adapted perturbation theory. *J. Chem. Phys.* **107**, 4207–4218. (doi:10.1063/1.474795)

23 Groenenboom, G. C., Wormer, P. E. S., van der Avoird, A., Mas, E. M., Bukowski, R. & Szalewicz, K. 2000 Water pair potential of near spectroscopic accuracy. II. Vibration–rotation–tunneling levels of the water dimer. *J. Chem. Phys.* **113**, 6702–6715. (doi:10.1063/1.1311290)

24 Smit, M. J., Groenenboom, G. C., Wormer, P. E. S., van der Avoird, A., Bukowski, R. & Szalewicz, K. 2001 Vibrations, tunneling, and transition dipole moments in the water dimer. *J. Phys. Chem. A* **105**, 6212–6225. (doi:10.1021/jp004609y)

25 Keutsch, F. N., Goldman, N., Harker, H. A., Leforestier, C. & Saykally, R. J. 2003 Complete characterization of the water dimer vibrational ground state and testing the VRT(ASP-W)III, SAPT-5st, and VRT(MCY-5f) surfaces. *Mol. Phys.* **101**, 3477–3492. (doi:10.1080/00268970310001636486)

26 Keutsch, F. N., Braly, L. B., Brown, M. G., Harker, H. A., Petersen, P. B., Leforestier, C. & Saykally, R. J. 2003 Water dimer hydrogen bond stretch, donor torsion overtone, and 'in-plane bend' vibrations. *J. Chem. Phys.* **119**, 8927–8937. (doi:10.1063/1.1614774)

27 Smit, M. J., Groenenboom, G. C., Wormer, P. E. S., van der Avoird, A., Bukowski, R. & Szalewicz, K. 2005 Vibrations, tunneling, and transition dipole moments in the water dimer. *J. Phys. Chem. A* **105**, 6212–6225. (doi:10.1021/jp004609y)

28 Bukowski, R., Szalewicz, K., Groenenboom, G. C. & van der Avoird, A. 2007 Predictions of the properties of water from first principles. *Science* **315**, 1249–1252. (doi:10.1126/science.1136371)

29 Scribano, Y. & Leforestier, C. 2007 Contribution of water dimer absorption to the millimeter and far infrared atmospheric water continuum. *J. Chem. Phys.* **126**, 234301. (doi:10.1063/1.2746038)

30 Bukowski, R., Szalewicz, K., Groenenboom, G. C. & van der Avoird, A. 2008 Polarizable interaction potential for water from coupled cluster calculations. I. Analysis of dimer potential energy surface. *J. Chem. Phys.* **128**, 094313. (doi:10.1063/1.2832746)
31 Bukowski, R., Szalewicz, K., Groenenboom, G. C. & van der Avoird, A. 2008 Polarizable interaction potential for water from coupled cluster calculations. II. Applications to dimer spectra, virial coefficients, and simulations of liquid water. *J. Chem. Phys.* **128**, 094314. (doi:10.1063/1.2832858)
32 Cencek, W., Szalewicz, K., Leforestier, C., van Harrevelt, R. & van der Avoird, A. 2008 An accurate analytic representation of the water pair potential. *Phys. Chem. Chem. Phys.* **10**, 4716–4731. (doi:10.1039/b809435g)
33 Szalewicz, K., Leforestier, C. & van der Avoird, A. 2009 Towards the complete understanding of water by a first-principles computational approach. *Chem. Phys. Lett.* **482**, 1–14. (doi:10.1016/j.cplett.2009.09.029)
34 Huang, X., Braams, B. J., Bowman, J. M., Kelly, R. E. A., Tennyson, J., Groenenboom, G. C. & van der Avoird, A. 2008 New *ab initio* potential energy and the vibration–rotation–tunneling levels of $(H_2O)_2$ and $(D_2O)_2$. *J. Chem. Phys.* **128**, 034312. (doi:10.1063/1.2822115)
35 Wormer, P. E. S. & van der Avoird, A. 2000 Intermolecular potentials, internal motions, and spectra of van der Waals and hydrogen-bonded complexes. *Chem. Rev.* **100**, 4109–4143. (doi:10.1021/cr990046e)
36 van der Avoird, A., Podeszwa, R., Szalewicz, K., Leforestier, C., van Harrevelt, R., Bunker, P. R., Schnell, M., von Helden, G. & Meijer, G. 2010 Vibration–rotation–tunneling states of the benzene dimer: an *ab initio* study. *Phys. Chem. Chem. Phys.* **12**, 8219–8240. (doi:10.1039/c002653k)
37 Kelly, R. E. A., Tennyson, J., Groenenboom, G. C. & van der Avoird, A. 2010 Water dimer vibration–rotation–tunnelling levels from vibrationally averaged monomer wavefunctions. *J. Quant. Spectrosc. Radiat. Transfer* **111**, 1262–1276. (doi:10.1016/j.jqsrt.2010.01.033)
38 Shank, A., Wang, Y., Kaledin, A., Braams, B. J. & Bowman, J. M. 2009 Accurate *ab initio* and 'hybrid' potential energy surfaces, intermolecular vibrational energies, and classical IR spectrum of the water dimer. *J. Chem. Phys.* **130**, 144 314. (doi:10.1063/1.3112403)
39 Thain, D., Tannenbaum, T. & Livny, M. 2005 Distributed computing in practice: the Condor experience. *Concurr. Comput. Pract. Exp.* **17**, 323–356. (doi:10.1002/cpe.938)
40 Calleja, M. *et al.* 2005 Collaborative grid infrastructure for molecular simulations: the eMinerals minigrid as a prototype integrated compute and data grid. *Mol. Sim.* **31**, 303–313. (doi:10.1080/08927020500067195)
41 Huang, Z. S. & Miller, R. E. 1989 High resolution near infrared spectroscopy of water dimer. *J. Chem. Phys.* **91**, 6613–6631. (doi:10.1063/1.457380)
42 Wang, Y., Shepler, B. C., Braams, B. J. & Bowman, J. M. 2009 Full-dimensional, *ab initio* potential energy and dipole moment surfaces for water. *J. Chem. Phys.* **131**, 054511. (doi:10.1063/1.3196178)
43 Shirin, S. V., Zobov, N. F., Ovsyannikov, R. I., Polyansky, O. L. & Tennyson, J. 2008 Water line lists close to experimental accuracy using a spectroscopically determined potential energy surface for $H_2{}^{16}O$, $H_2{}^{17}O$ and $H_2{}^{18}O$. *J. Chem. Phys.* **128**, 224306. (doi:10.1063/1.2927903)
44 Tennyson, J., Kostin, M. A., Barletta, P., Harris, G. J., Polyansky, O. L., Ramanlal, J. & Zobov, N. F. 2004 DVR3D: a program suite for the calculation of rotation–vibration spectra of triatomic molecules. *Comput. Phys. Commun.* **163**, 85–116. (doi:10.1016/j.cpc.2003.10.003)
45 Shirin, S. V., Polyansky, O. L., Zobov, N. F., Barletta, P. & Tennyson, J. 2003 Spectroscopically determined potential energy surface of $H_2{}^{16}O$ up to 25000 cm^{-1}. *J. Chem. Phys.* **118**, 2124–2129. (doi:10.1063/1.1532001)
46 Barletta, P., Shirin, S. V., Zobov, N. F., Polyansky, O. L., Tennyson, J., Valeev, E. F. & Csaszar, A. G. 2006 CVRQD *ab initio* ground-state adiabatic potential energy surfaces for the water molecule. *J. Chem. Phys.* **125**, 204307. (doi:10.1063/1.2378766)
47 Le Sueur, C. R., Miller, S., Tennyson, J. & Sutcliffe, B. T. 1992 On the use of variational wavefunctions in calculating vibrational band intensities. *Mol. Phys.* **76**, 1147–1156. (doi:10.1080/00268979200101941)

48 Henderson, J. R., Le Sueur, C. R. & Tennyson, J. 1993 DVR3D: programs for fully pointwise calculation of vibrational spectra. *Comput. Phys. Commun.* **75**, 379–395. (doi:10.1016/0010-4655(93)90050-M)
49 Lodi, L. *et al.* 2008 A high accuracy dipole surface for water. *J. Chem. Phys.* **128**, 044304. (doi:10.1063/1.2817606)
50 Lodi, L., Tennyson, J. & Polyansky, O. L. 2011 A global, high accuracy *ab initio* dipole moment surface for the electronic ground state of the water molecule. *J. Chem. Phys.* **135**, 034113. (doi:10.1063/1.3604934)
51 Buck, U. & Huisken, F. 2000 Infrared spectroscopy of size-selected water and methanol clusters. *Chem. Rev.* **100**, 3863–3890. (doi:10.1021/cr990054v)
52 Bouteiller, Y. & Perchard, J. P. 2004 The vibrational spectrum of $(H_2O)_2$: comparison between anharmonic *ab initio* calculations and neon matrix infrared data between 9000 and 90 cm^{-1}. *Chem. Phys.* **305**, 1–12. (doi:10.1016/j.chemphys.2004.06.028)
53 Paul, J. B., Provencal, R. A., Chapo, C., Roth, K., Casaes, R. & Saykally, R. J. 1999 Infrared cavity ringdown spectroscopy of the water cluster bending vibrations. *J. Phys. Chem. A* **103**, 2972–2974. (doi:10.1021/jp984618v)
54 Paynter, D. J., Ptashnik, I. V., Shine, K. P., Smith, K. M., McPheat, R. & Williams, R. G. 2009 Laboratory measurements of the water vapor continuum in the 1200–8000 cm^{-1} region between 293 K and 351 K. *J. Geophys. Res.* **114**, D21301. (doi:10.1029/2008JD011355)
55 Kuyanov-Prozument, K., Choi, M. Y. & Vilesov, A. 2010 Spectrum and infrared intensities of OH-stretching bands of water dimers. *J. Chem. Phys.* **132**, 014304. (doi:10.1063/1.3276459)
56 Bouteiller, Y., Tremblay, B. & Perchard, J. P. 2011 The vibrational spectrum of the water dimer: comparision between anharmonic *ab initio* calculations and neon matrix infrared data between 14,000 and 90 cm^{-1}. *Chem. Phys.* **386**, 29–40. (doi:10.1016/j.chemphys.2011.05.014)